COMPARISON OF REGIONAL MYOCARDIAL FUNCTION IN THE HUMAN AND THE MOUSE

C. Constantinides[1], D. Rueckert[2], and D. Perperidis[1]
[1]Mechanical and Manufacturing Engineering, University of Cyprus, Nicosia, Cyprus, [2]Imperial College London, London, United Kingdom

Introduction: While cardiac functional studies initially focused on large mammals and humans, the mouse has emerged as the preferred animal species for such research in recent years. With the completion of the mouse and human genome mapping, a plethora of mouse studies emerged with genetic modifications targeting the cardiovascular system in mice to investigate human disease. MRI techniques (tagging, harmonic phase imaging, and DENSE) have been used over the last decade to quantify cardiac function, allowing myocardial tracking, motion and strain quantification, in normal and genetically engineered mice [1-3]. Critical to such work is the validation of the underlying hypothesis of functional scaling from mouse to human (through consideration of global cardiac function, circulatory control, blood flow distribution, Ca^{2+} storage and cycling, myocin light chain distribution, and force frequency reserve) for comparative studies. The goals of this study were to quantify and compare regional and global cardiac performance in humans and mice. Such work has potential clinical significance in mouse phenotyping for determining myocardial dysfunction, in correlation with perfusion and metabolism.

Methods: *Human Imaging:* Eight human volunteers [7 male (age range=25-35 years); one female (age=28 years)] were imaged (with informed consent). All studies were approved by the Institutional Review Board at Imperial College. All imaging for the human work was conducted on a Siemens Sonata 1.5 T scanner using a TrueFisp pulse sequence. Image pixel size ranged from [1.36-1.48x1.36-1.48] mm^2, and the slice thickness was 10 mm. For these subjects 15-20 different cardiac frames were acquired throughout the cardiac cycle (R-R intervals ranged from 600-800 ms). *Mouse Imaging:* Nine C57BL/6J (weight±sd=23.3±5.6 g; age=8-12.5 weeks) mice were imaged under isoflurane anesthesia conditions using a 7T GE scanner and a custom-made 2.5x3cm^2 transmit/receive surface coil at Duke. A 4D radial pulse sequence was used with TE=300μs, TR=2.4ms, BW=±125kHz, flip angle=45, temporal resolution of 9.6ms, spatial resolution of 110$μm^3$, 8 cardiac phases, in 31 minutes. *Image Processing: Quantification of Global Cardiac Function*: 3D volume renditions of the left (LV) ventricular cavity were generated by two expert users using Vitrea (Vital Image Inc, USA) and the LV blood cavity volume curves estimated. Estimated LV preload (EDV) and end-systolic volumes (ESV) were converted to absolute volume by appropriate image voxel scaling. Myocardial mass, stroke volume (SV), ejection fractions (EF), cardiac output (CO) were calculated according to: SV=EDV-ESV, EF=SV/EDV, and CO=HR.SV, where HR is the heart rate. *Quantification of Regional Cardiac Function*: Voxel displacement maps were generated from user-defined epicardial and endocardial border definition using splines, throughout the cardiac cycle, and the subsequent estimation of wall thickening (WT), wall motion (WM), and regional ejection fraction (rEF) using Vitrea, according to:

$$Wall\,Motion = ED_{epicardial\_wall\_diameter} - ES_{epicardial\_wall\_diameter},\ Wall\,Thickening = 100.\frac{\left(ES_{wall\_thickness} - ED_{wall\_thickness}\right)}{ED_{wall\_thickness}},\ rEF = 100.\frac{\left(ED_{endocardial\_diameter}^{\ 2} - ED_{endocardial\_diameter}^{\ 2}\right)}{ED_{endocardial\_diameter}^{\ 2}}$$

A 17-sector bulls-eye representation was subsequently used to graphically present such results.

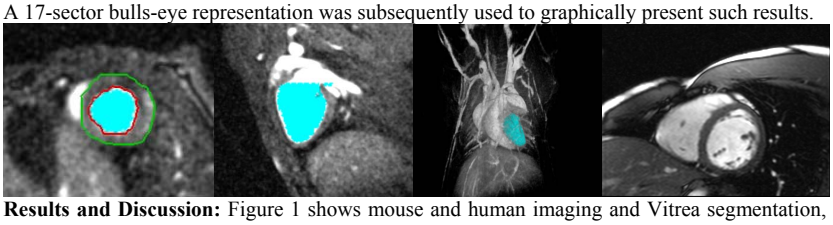

Figure 1: *(Left to right) Epicardial and endocardial LV contour definition in mouse short and long-axis MRI, and 3D LV blood cavity segmentation; 3D ventriculogram rendition using Vitrea from murine MRI; short axis human MRI.*

Results and Discussion: Figure 1 shows mouse and human imaging and Vitrea segmentation, while Figure 2 depicts typical bullseye sectoral plots for wall motion, wall thickness, and rEF in mouse and humans. Quantification of regional functional parameters of the mouse and human are shown in Figure 3 and tabulated in Table 1. Similar spatial patterns were observed for mouse and human (in agreement with prior tagging work [1]) supported by two-tailed paired t-tests indicating no statistical significant difference in the mean values of wall thickness (p=0.07), wall motion (p=0.051), or rEF (p=0.065) at the 1% significance. Repeated measures ANOVA indicated significant difference in regional mouse and human for WT (p=0.002) and rEF (p<0.0001) and insignificant differences for WM (p=0.016) at 1% significance. Comparative to prior reports of global functional indices [4,5], similar mouse and human results were also observed. The work supports the validity of the hypothesis of functional scaling in mice and humans.

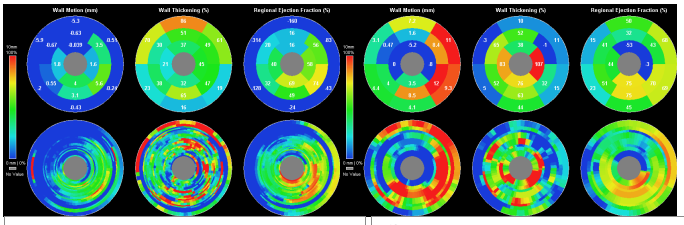

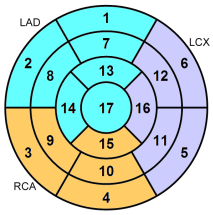

Figure 2: (Left) *Wall motion, wall thickness, and rEF in bullseye plot representation for a typical mouse (Left), and a typical human dataset (Middle);(Right) LV sectoral representation.*

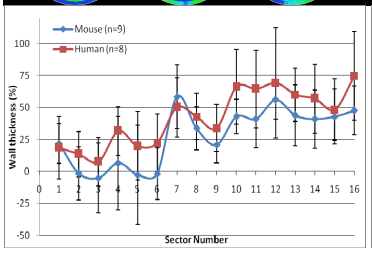

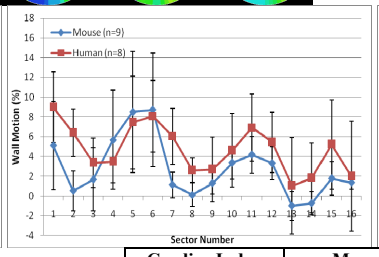

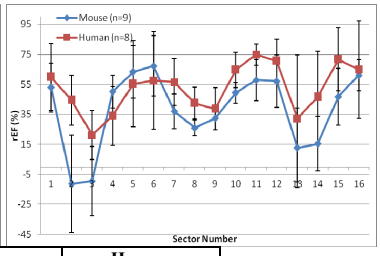

Figure 3: *Wall thickness, wall motion, and rEF variation in the various sectors of the murine and human myocardium.*

Cardiac Index	Mouse	Human
EF	50.7±3.7 %	64.4±2.4 %
EDV	45.4±11.0 μl	117±32.7 ml
ESV	22.5±6.2 μl	46.5±10.3 ml
SV	22.9±5.4 μl	83±15.4 ml
CO	1.4±0.3 ml/min	5.0±0.9 l/min
Myocardial Mass	-	153.1±37.2 g
rEF	38.0±25.0 %	52.2±15.8 %
Wall Motion	2.8±3.0 %	4.8±2.4 %
Wall Thickness	27.9±22.4 %	42.6±21.8 %

Table 1*: Summary of mean global and regional cardiac mechanical functional indices (±sd) of murine and human myocardium.*

References: **1**) Moore CC et al. Radiology 214:453-466, 2000. **2**) Osman NF et al. IEEE TBE 51:1428-1433, 2004. **3**) Aletras A et al. J Magn Reson 137:247-252, 1999. **4**) Bucholz E, et al. MRM 63(4):979-987, 2010. **5**) Brandts A, et al. 64:1472-1479, 2010.

Acknowledgements: Mouse imaging was performed at the Duke Center for In Vivo Microscopy, supported by NCRR (P41 RR005959/U24 and NCI CA092656). Funding was received from grants 'HEART' (Hellenic Bank) and STOXOS0308/02, PROSVASI0308/01 from the Research Promotion Foundation.